BJP British Journal of Pharmacology

DOI:10.1111/bph.12336
www.brjpharmacol.org

RESEARCH PAPER

Crucial roles of Nox2-derived oxidative stress in deteriorating the function of insulin receptors and endothelium in dietary obesity of middle-aged mice

Junjie Du[1]*, Lampson M Fan[2]*, Anna Mai[1] and Jian-Mei Li[1]

[1]*Faculty of Health and Medical Sciences, University of Surrey, Guildford, UK, and* [2]*John Radcliffe Hospital, University of Oxford, Oxford, UK*

Correspondence
Professor Jian-Mei Li, Faculty of Health and Medical Sciences, University of Surrey, AY Building, Guildford, Surrey GU2 7XH, UK.
E-mail: j.li@surrey.ac.uk

*Equal contribution of these two authors.

Statement of author contributions: J.D. research data; L.M.F. research data, wrote the manuscript; A.M. research data; J-M.L. directed and financed the research, research data, review/edited manuscript.

Keywords
obesity; insulin resistance; ageing; endothelial dysfunction; Nox2 inhibitor; NADPH oxidase; oxidative stress

Received
11 June 2013
Revised
5 August 2013
Accepted
8 August 2013

BACKGROUND AND PURPOSE
Systemic oxidative stress associated with dietary calorie overload plays an important role in the deterioration of vascular function in middle-aged patients suffering from obesity and insulin resistance. However, effective therapy is still lacking.

EXPERIMENTAL APPROACH
In this study, we used a mouse model of middle-aged obesity to investigate the therapeutic potential of pharmaceutical inhibition (apocynin, 5 mM supplied in the drinking water) or knockout of Nox2, an enzyme generating reactive oxygen species (ROS), in high-fat diet (HFD)–induced obesity, oxidative stress, insulin resistance and endothelial dysfunction. Littermates of C57BL/6J wild-type (WT) and Nox2 knockout (KO) mice (7 months old) were fed with a HFD (45% kcal fat) or normal chow diet (NCD, 12% kcal fat) for 16 weeks and used at 11 months of age.

KEY RESULTS
Compared to NCD WT mice, HFD WT mice developed obesity, insulin resistance, dyslipidaemia and hypertension. Aortic vessels from these mice showed significantly increased Nox2 expression and ROS production, accompanied by significantly increased ERK1/2 activation, reduced insulin receptor expression, decreased Akt and eNOS phosphorylation and impaired endothelium-dependent vessel relaxation to acetylcholine. All these HFD-induced abnormalities (except the hyperinsulinaemia) were absent in apocynin-treated WT or Nox2 KO mice given the same HFD.

CONCLUSIONS AND IMPLICATIONS
In conclusion, Nox2-derived ROS played a key role in damaging insulin receptor and endothelial function in dietary obesity after middle-age. Targeting Nox2 could represent a valuable therapeutic strategy in the metabolic syndrome.

Abbreviations
DHE, dihydroethidium; DPI, diphenyleneiodonium; EFP, epididymal fat pad; HFD, high-fat diet; IPGTT, intraperitoneal glucose tolerance test; IR, insulin receptor; KO, knockout; MnTMPyP, Mn(III)tetrakis(1-methyl-4-pyridyl)porphyrin; NCD, normal chow diet; ROS, reactive oxygen species; WT, wild-type

Introduction

The obesity epidemic has become a major public health problem around the world. At least one in two people are now considered to be overweight or obese in most Western countries (Parikh *et al.*, 2007; Houston *et al.*, 2009). Obesity along with other metabolic disorders such as insulin resistance, dyslipidaemia, impaired glucose tolerance and hypertension, is referred to as the metabolic syndrome or pre-diabetes (Evans *et al.*, 2002; Furukawa *et al.*, 2004; Gupta *et al.*, 2012). The highest prevalence of obesity is among the middle aged who commonly also have insulin resistance and type 2 diabetes resulting in increased cardiovascular morbidity and mortality (Parikh *et al.*, 2007; Houston *et al.*, 2009; Bailey, 2011). One of the main contributors to the obesity epidemic is the consumption of food rich in dietary fat. Although several factors are involved, considerable evidence has suggested that a high-fat diet (HFD) leads to the development of the metabolic syndrome through the activation of an $O_2^{\cdot-}$-generating NADPH oxidase 2 (Nox2) and systemic (or multiorgan) oxidative stress (Evans *et al.*, 2002; Furukawa *et al.*, 2004; Sonta *et al.*, 2004; Silver *et al.*, 2007; Sukumar *et al.*, 2013). Indeed, a clinical study had shown that in obese patients there was up-regulation of platelet Nox2 expression and increased oxidative stress as indicated by increased levels of urinary isoprostanes and serum oxidized-low density lipoprotein (LDL) (Violi *et al.*, 2009).

The Nox family has seven members, namely Nox1–5 and Duox 1–2, and among them, Nox2 is also known as $gp91^{phox}$ (Sumimoto *et al.*, 2005). The Nox2 enzyme contains a cytochrome b_{558} (consisting of a Nox2 and a $p22^{phox}$), and at least four regulatory subunits, including $p40^{phox}$, $p47^{phox}$, $p67^{phox}$ and Rac1. In the vasculature, Nox2 is expressed in the endothelial cells and adventitial fibroblasts, and very little was detected (if any) in smooth muscle cells (Lassègue and Clempus, 2003; Li and Shah, 2004). In terms of diabetes, Nox2 has been found to play a critical role in HFD or high glucose-induced beta-cell dysfunction (Yuan *et al.*, 2010), oxidative stress and vascular dysfunction (Hink *et al.*, 2001). Nox2 is a major source of endothelial reactive oxygen species (ROS) production in response to TNFα, high levels of glucose, LDL cholesterol and free fatty acid (FFA) stimulation (Li *et al.*, 2002; 2005; Furukawa *et al.*, 2004; Silver *et al.*, 2007). Endothelial dysfunction due to the excessive ROS production by Nox2 predisposes to cardiovascular complications in obesity. Accordingly, the purpose of the present study was to investigate the therapeutic potential of inhibition or knockout (KO) of Nox2 in the improvement of obesity-related metabolic syndrome and endothelial function after middle age.

Apocynin has been widely used experimentally as a naturally occurring inhibitor of the Nox2 enzyme with anti-inflammatory effects (Touyz, 2008). However, apocynin has also been reported to be an antioxidant rather than a specific Nox2 inhibitor in the vascular system (Heumüller *et al.*, 2008). In streptozotocin-induced type 1 diabetes, apocynin normalized cardiac NADPH oxidase activity *in vivo* (Oelze *et al.*, 2011), and improved endothelial function *ex vivo* (Lopez-Lopez *et al.*, 2008). In diet-induced obesity and insulin resistance, apocynin improved the symptoms of metabolic disorder, although it was unclear if this effect was exerted through its antioxidative properties or due to inhibition of Nox2 (Sonta *et al.*, 2004; Meng *et al.*, 2010).

In the current study, we generated a mouse model of middle-aged (11 months) dietary obesity, using age-matched wild-type (WT) and Nox2 knockout (Nox2KO) mice on the C57BL/6J background. We treated the HFD WT mice with apocynin and compared the effects of apocynin-treatment with Nox2KO given the same diet. Our study demonstrated for the first time a crucial role for Nox2 in dietary obesity-related vascular oxidative stress and oxidative damage of vascular insulin receptors (IR) and endothelial function.

Methods

Animals and dietary treatment

All animal care and experimental procedures complied with the protocols approved by the Home Office under the Animals (Scientific Procedures) Act 1986, UK and the local Animal Ethics Committee of University of Surrey. All studies involving animals are reported in accordance with the ARRIVE guidelines for reporting experiments involving animals (Kilkenny *et al.*, 2010; McGrath *et al.*, 2010). A total of 90 animals was used in the experiments described here. Littermates of WT and Nox2KO mice on C57BL/6J background (Jackson Laboratory, Bar Harbor, ME, USA) were bred in our institution from heterozygotes and genotyped. Male mice at 7 months of age were randomly assigned (n = 18/per group) to a HFD: 45% kcal fat, 20% kcal protein and 35% kcal carbohydrate (Special Diets Services, Essex, UK), or a normal chow diet (NCD): 9.3% kcal fat, 25.9% kcal protein, and 64.8% kcal carbohydrate (LabDiet Ltd, London, UK) for 16 weeks. Apocynin was supplied in drinking water (5 mM). Body weights were measured weekly. Mice (at 11 months) were fasted 8 h before being killed by overdose of pentobarbital. The body weight and the epididymal fat pad (EFP) weight were recorded.

Metabolic measurements and intraperitoneal glucose tolerance test (IPGTT)

Venous blood samples (0.5 mL) were taken at 0900 h after 8 h of fasting. Glucose was measured using a blood glucose meter (Contour, Bayer HealthCare, Newbury, UK). Plasma insulin was measured using a mouse insulin enzyme-linked immunosorbent assay kit (Mercodia Developing Diagnostic, Uppsala, Sweden). Insulin resistance was calculated using the homeostasis model assessment of insulin resistance (HOMA-IR). The fasting serum cholesterol, FFA, triglyceride and high-density-lipoprotein (HDL) cholesterol were measured by enzymatic colorimetric assays using the ILab 650 Chemistry Systems (Instrumentation Laboratory, Cheshire, UK). The LDL cholesterol was calculated as the difference between total and HDL cholesterol concentrations based on the Friedewald equation (Abudu and Levinson, 2007). For the IPGTT, mice were fasted for 8 h, and a solution of glucose (2 $g \cdot kg^{-1}$ body weight) was injected i.p. and blood glucose measured at 15, 30, 60 and 120 min after injection.

Blood pressure (BP) and endothelial function assessments

BP was measured by a computer controlled, non-invasive, tail-cuff BP system (Kent Scientific Corporation, Torrington,

CT, USA) on conscious mice at 1000 h. Mice were trained for 5 days to be habituated to the instrument. The measurement was recorded by the CODA™ program and the mean of at least six successful recordings was used for each mouse.

For assessing the endothelial function, freshly isolated thoracic aorta rings were cut 3–4 mm long and suspended in an organ bath (ML0146/C-V, AD Instrument Ltd, Colorado Springs, CO, USA) containing 10 mL (37°C) of Krebs-Henseleit solution (in mM: NaCl 118, KCl 4.7, KH_2PO_4 1.2, $MgSO_4$ 1.2, $CaCl_2$ 2.5, $NaHCO_3$ 25, glucose 12, pH 7.4) gassed with 95% O_2/5% CO_2 (Fan *et al.*, 2009). The maximal contractile response to KCl (50 mM) was assessed firstly. After washout and re-equilibration, endothelium-dependent relaxation to acetylcholine (ACh, 0.001–10 μM added cumulatively) and endothelium-independent vessel relaxation to sodium nitroprusside (SNP, 0.0001–1 μM added cumulatively) were tested in rings preconstricted with phenylephrine (0.001–10 μM added cumulatively) to 70% of their maximal phenylephrine-induced contractile response. In some experiments, the vessels were pre-incubated with tiron (a non-enzymatic $O_2^{\cdot-}$ scavenger; 10 mM, 15 min) or the NOS inhibitor L-NAME, (100 μM for 30 min), or endothelial denudation. To assess the effect of insulin on vessel contractile response to phenylephrine, we pre-incubated aortas with or without insulin (1.2 nM) for 2 h before assessing the response to phenylephrine (Wheatcroft *et al.*, 2004). Production of NO was assessed by measuring the concentration of serum nitrite, which is one of the primary stable and non-volatile breakdown products of NO, using the Griess assay kit from Promega (Southampton, UK).

Organ culture of aorta

Aortas from 11-month-old NCD WT and Nox2KO mice were cut into 4 mm rings and incubated at 37°C for 24 h in a cell culture incubator in the control medium (2% FCS/DMEM) or stimulated with insulin (1.2 nM) and high glucose (40 mM) to mimic the condition of insulin-resistance in the presence or absence of apocynin (100 μM) or an inhibitor of ERK1/2 activation (U0126, 10 μM). Homogenates of the aorta were used for immunoblotting for the expression of insulin receptor and ERK1/2 and eNOS phosphorylation.

ROS measurement

Production of $O_2^{\cdot-}$ by aortic tissue homogenates was measured by lucigenin (5 μM)-chemiluminescence (Lumistar, BMG Labtech GmbH, Ortenberg, Germany) as described previously (Teng *et al.*, 2012). The specificity of $O_2^{\cdot-}$ was confirmed by adding tiron (10 mM) to scavenge the $O_2^{\cdot-}$. The enzymatic sources of $O_2^{\cdot-}$ production were identified using inhibitors targeting NOS (L-NAME 100 μM), the mitochondrial complex-1 enzymes (rotenone, 50 μM), xanthine oxidase (oxypurinol, 250 μM), flavo-proteins [diphenyleneiodonium, (DPI), 20 μM], or superoxide dismutase (SOD; 200 U·mL^{-1}) before $O_2^{\cdot-}$ measurement. As an alternative approach, *in situ* generation of ROS in aorta sections was measured by DHE fluorescence (Li *et al.*, 2004). Briefly, cryosections (20 μM) of fresh aortic tissues were equilibrated for 30 min at 37°C in Krebs-HEPES buffer. DHE (2 μM) was then applied in the presence or absence of tiron (10 mM) and incubated in the dark for 10 min. Images were captured digitally and acquired using Olympus BX61 fluorescence microscope. The fluorescence intensity was quantified from at least five random fields (269.7 × 269.2 μm) per section with three sections per sample and six animals per group.

Immunoblotting

Immunoblotting using 40 μg protein per lane was performed as described previously (Thakur *et al.*, 2010). The images were captured digitally using a BioSpectrum AC imaging system (UVP, Cambridge, UK), and the optical densities of the protein bands were normalized to the loading control bands and quantified.

Immunofluorescence microscopy

The experiments were performed exactly as described previously (Thakur *et al.*, 2010). Briefly, frozen sections (6 μm) were firstly treated with a biotin blocking kit (DAKO UK Ltd, Cambridgeshire, UK). Primary antibodies (1:250 dilution) were incubated with the sections for 1 h at room temperature. Biotin-conjugated anti-rabbit or anti-goat IgG (1:1000 dilution) were used as secondary antibodies. Specific binding was detected by extravidin-FITC or streptavidin-Cy3. Normal rabbit or goat IgG (5 μg·mL^{-1}) was used instead of primary antibody as a negative control. Images were acquired with an Olympus BX61 fluorescence microscope system. Fluorescence intensities were quantified as described above.

Data analysis

The data are expressed as the means ± SD from 6 to 18 mice per group. Statistical analysis was performed with one-way or two-way ANOVA, followed by Bonferroni post tests. $P < 0.05$ was considered statistically significant.

Materials

Polyclonal antibodies against $p22^{phox}$, Nox1, Nox2, Nox4, $p40^{phox}$, $p47^{phox}$, $p67^{phox}$, Rac1, IRα, IRβ and phospho-eNOS-Ser^{1177} were from Santa Cruz Biotechnology (Dallas, TX, USA). Antibodies to phospho-ERK1/2, phospho-p38MAPK, phospho-JNK and phospho-Akt-Ser^{473} were from Cell Signalling Technology (Danvers, MA, USA). Dihydroethidium (DHE) was from Invitrogen (Paisley, UK). Apocynin and other reagents were from Sigma (Dorset, England) unless stated otherwise.

Results

The effects of apocynin treatment or Nox2KO on HFD-induced obesity and metabolic syndrome

Before diet intervention, there was no significant difference in body weight, food and water intakes between WT and Nox2KO mice at 7 months of age (Table 1). After 16 weeks of diet intervention (at 11 months of age), there was no significant difference in daily food intake between groups given the same diet except that the HFD mice were eating less food (equal energy intake) than the NCD controls. HFD WT mice showed significant increases of body weight (Figure 1A), EFP weight, levels of fasting serum triglycerides, FFA, total and LDL cholesterols; and of BP (Figure 1B). All these HFD-related metabolic abnormalities were significantly improved and the

Table 1

Pathophysiological measurements before and after diet intervention

Parameter	16 weeks diet	Wild-type (WT) NCD	Wild-type (WT) HFD	Wild-type (WT) HFD+ apocynin	Nox2KO NCD	Nox2KO HFD
Body weight (g)	Before	34.5 ± 1.9	33.8 ± 1.5	35.6 ± 2.1	34.0 ± 1.7	34.6 ± 2.5
	After	42.2 ± 1.8	56.4 ± 3.1*	48.4 ± 2.2#	40.0 ± 3.5	49.1 ± 4.0*†
Epididymal fat pad weight (g)	After	1.08 ± 0.30	2.56 ± 0.21*	1.45 ± 0.34#	1.28 ± 0.46	1.73 ± 0.19*†
Heart weight (mg)	After	171 ± 11	182 ± 19	173 ± 20	171 ± 20	177 ± 25
Food intake (g·day^{-1})	Before	3.69 ± 0.15	3.66 ± 0.55	3.63 ± 0.62	3.72 ± 0.52	3.10 ± 0.67
	After	3.53 ± 0.26	2.70 ± 0.43*	2.75 ± 0.68	3.37 ± 0.48	2.56 ± 0.40*
Energy intake (kcal·day^{-1})	Before	11.24 ± 0.50	12.15 ± 1.83	12.05 ± 2.05	12.34 ± 1.74	10.30 ± 2.21
	After	11.71 ± 0.86	12.25 ± 1.96	12.46 ± 3.08	11.20 ± 1.59	11.60 ± 1.81

Results were presented as mean ± SD of 13 mice per group.
*$P < 0.05$, significantly different from normal chow diet (NCD).
#$P < 0.05$, significantly different from high-fat diet (HFD).
†$P < 0.05$, significant differences between Nox2KO (knockout) and corresponding WT values.

BP was maintained within the normal range in apocynin-treated HFD WT mice (Figure 1B). However, in Nox2KO mice, HFD only induced mild increases in body weight and the levels of total and LDL cholesterols. The EFP/body weight ratio, serum fasting triglycerides and FFA, and BP in HFD Nox2KO mice stayed at the levels of their NCD controls.

WT mice under HFD had significantly higher levels of fasting serum glucose and insulin with high scores of HOMA-IR indicating insulin resistance (Figure 2A). Interestingly, apocynin-treated WT HFD mice or Nox2KO mice under HFD had also elevated serum levels of fasting insulin, but their glucose levels were significantly reduced, compared with the HFD WT mice (Figure 2A). Improved glucose tolerance was further confirmed by the IPGTT assays. This test was impaired in HFD WT mice but well preserved in apocynin-treated WT and Nox2KO mice under HFD (Figure 2B). We also measured the serum concentration of nitrite (a final product of NO breakdown) as an index of systemic NO production, and found a significant reduction of serum nitrite in HFD WT mice suggesting NOS dysfunction, but not in apocynin-treated WT and Nox2KO mice (Figure 2C).

HFD-induced aorta Nox2 up-regulation, oxidative stress and redox-sensitive MAPK activation

HFD WT aortas had significantly higher levels of NADPH-dependent $O_2^{\cdot-}$ production, which were decreased to the NCD WT levels by treatment with apocynin (Figure 2D). In contrast, in Nox2KO aortas, the levels of NADPH-dependent $O_2^{\cdot-}$ production were very low in both HFD and NCD mice, without significant differences. Tiron was used to confirm the detection of $O_2^{\cdot-}$. The enzymatic sources of $O_2^{\cdot-}$ production in HFD WT aortas were further examined using different enzyme inhibitors (Figure 2D, lower panel). The production of this ROS was inhibited significantly by SOD and DPI (a flavo-protein inhibitor), but not by rotenone (mitochondria complex 1 enzyme inhibitor) or oxypurinol (xanthine oxidase inhibitor) further supporting Nox2 as a major enzymatic source of the HFD-induced vascular $O_2^{\cdot-}$ production. However, L-NAME (NOS inhibitor) also inhibited slightly, but significantly (~20%), the $O_2^{\cdot-}$ production by HFD WT aorta homogenates, suggesting some dysfunction of eNOS.

To define a role of Nox in HFD-induced vascular oxidative stress and dysfunction, we examined, in extracts of aorta, the protein expression of Nox1, Nox2, Nox4, $p22^{phox}$ and the regulatory subunits of Nox2 that are $p40^{phox}$, $p47^{phox}$, $p67^{phox}$ and Rac1 by immunoblotting (Figure 3A). Compared to NCD WT controls, HFD WT aortas had significantly higher levels of Nox2, $p22^{phox}$, $p40^{phox}$, $p47^{phox}$ $p67^{phox}$ and Rac1, and these high levels were restored to the NCD levels by apocynin treatment. However the high levels of Nox2 were not affected indicating that apocynin did not change Nox2 expression. The levels of Nox1 and Nox4 were not significantly affected by HFD intervention (Figure 3A). We then examined HFD-induced MAPK activation using monoclonal antibodies against phospho-ERK1/2, phospho-p38MAPK and phospho-JNK (Figure 3B), and found that HFD induced significant increases in ERK1/2 and p38MAPK phosphorylation in WT aortas, but not in apocynin-treated or in HFD-Nox2KO aortas (Figure 3B). The levels of phosphorylated JNK were very low without significant changes. The total protein levels of ERK1/2, p38MAPK, and JNK in the same samples were used as loading controls.

The effects of Nox2-derived oxidative stress on aorta insulin receptor expression, Akt and eNOS phosphorylation and endothelial function

To explore the relationship between Nox2–derived oxidative stress, vascular insulin-resistance and endothelial dysfunction, we examined the expression of IRα and IRβ by immunoblotting. HFD reduced significantly the protein levels of both IRα and IRβ in WT aortas, but not in apocynin-treated or HFD-Nox2KO aortas (Figure 4A, left panel). We then examined phosphorylation of Akt, which is an signalling molecule

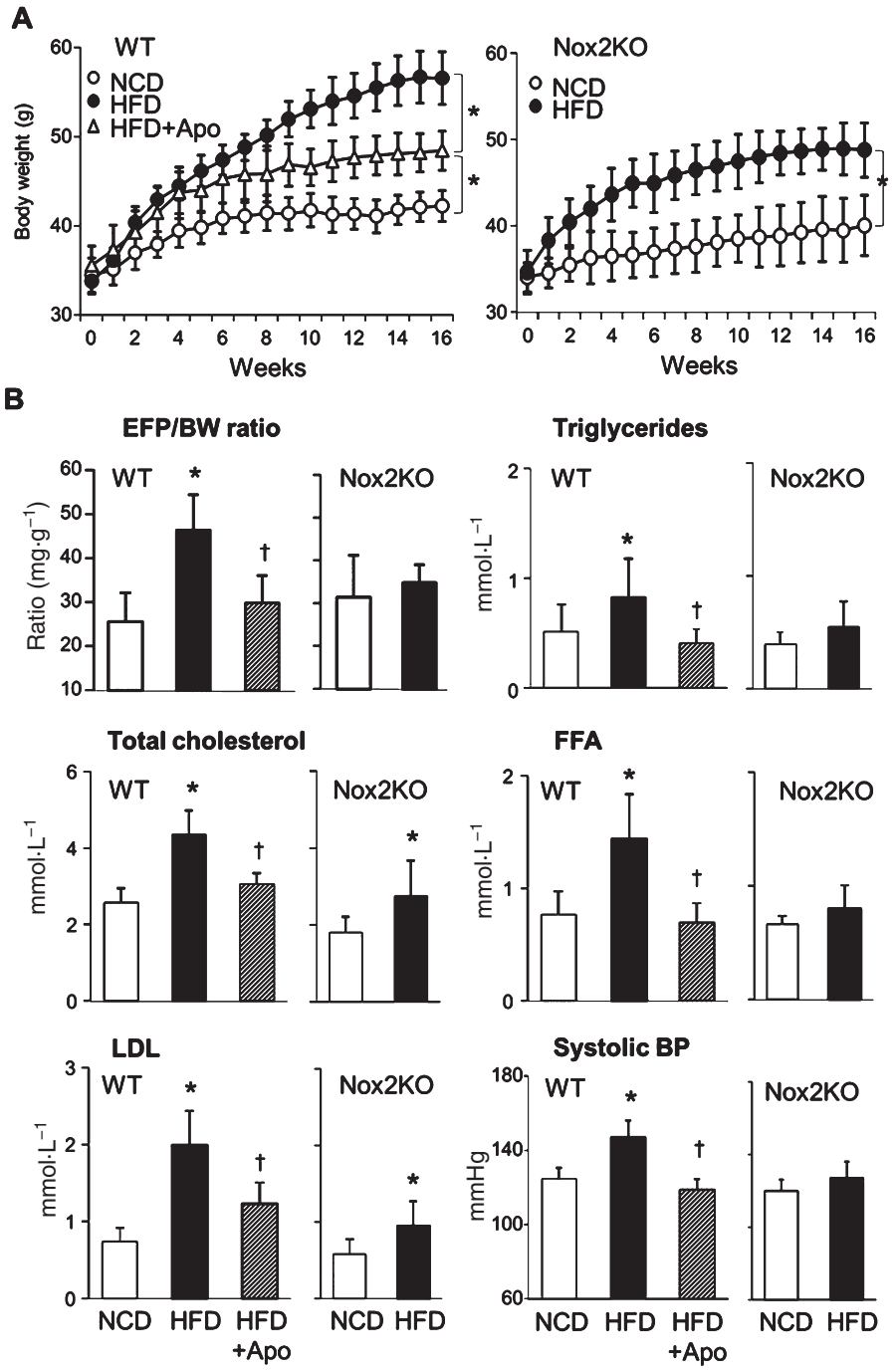

Figure 1

High-fat diet (HFD)-induced metabolic changes in wild-type (WT) and Nox2KO mice. (A) Body weight (BW) increases; (B) Changes in the epididymal fat pad (EFP)/BW ratio; fasting serum triglycerides, total and LDL cholesterol; FFA and systolic BP after 16 weeks of diet intervention. *$P < 0.05$, significantly different from normal chow diet (NCD) values. †$P < 0.05$, significantly different from HFD values. $n = 13$ mice per group.

downstream of IR, and found that Akt phosphorylation was significantly reduced in HFD WT aortas, but remained at the NCD control level in apocynin-treated or HFD-Nox2KO aortas (Figure 4A, middle panel). Akt phosphorylates eNOS at Ser^{1117} and we therefore examined the eNOS phosphorylation by immunoblotting. We found that Ser^{1117} phosphorylation of eNOS was significantly decreased in HFD WT aortas but remained at the NCD control levels in apocynin-treated or HFD-Nox2KO aortas (Figure 4A, right panel).

We examined next the endothelial function. Compared to NCD WT controls, the endothelium-dependent relaxation of aortic rings to acetylcholine was attenuated in HFD WT aortas, and this was prevented by apocynin treatment (Figure 4B) or by Nox2KO (Figure 4C). The relaxation to

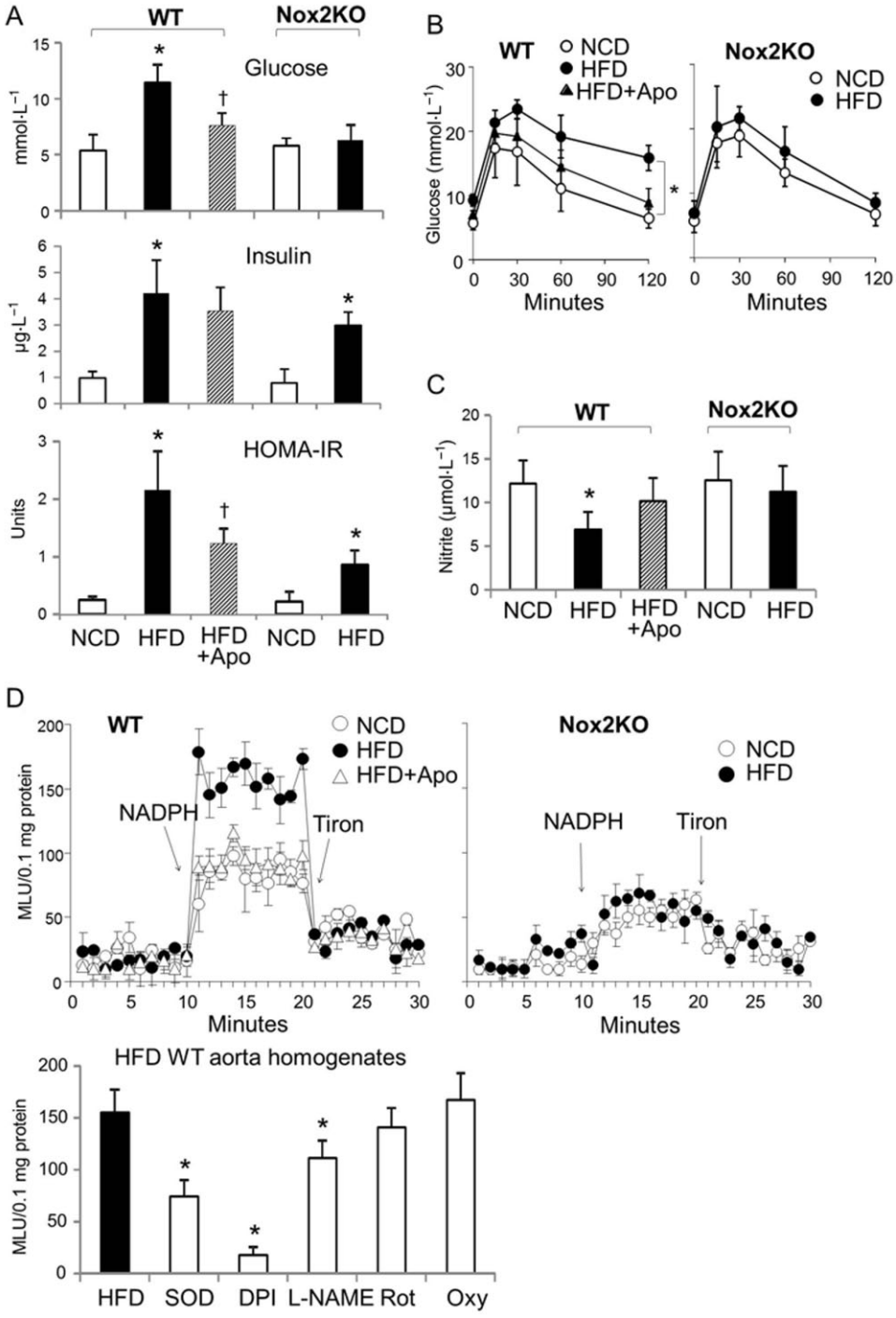

Figure 2

High-fat diet (HFD)-induced changes in the levels of fasting serum glucose, insulin, nitrite, intraperitoneal glucose tolerance test (IPGTT) and aorta reactive oxygen species (ROS) production in wild-type (WT) and Nox2KO mice. (A) Levels of fasting serum glucose, fasting insulin and calculated HOMA-IR values; (B) Glucose tolerance test; (C) Serum nitrite concentration. *$P < 0.05$, significantly different from normal chow diet (NCD) values. †$P < 0.05$, significantly different from HFD values. (D) $O_2^{\cdot-}$ production detected by lucigenin-chemiluminescence. Upper panels: Kinetic measurement of $O_2^{\cdot-}$ production. NADPH was added at 10 min. Tiron was added at 20 min. Lower panel: the effect of different enzyme inhibitors on $O_2^{\cdot-}$ production by HFD WT aorta homogenates; SOD, superoxide dismutase; DPI, diphenylene iodonium; Rot, rotenone; Oxy, oxypurinol. *$P < 0.05$, significantly different from HFD values. $n = 13$ mice per group.

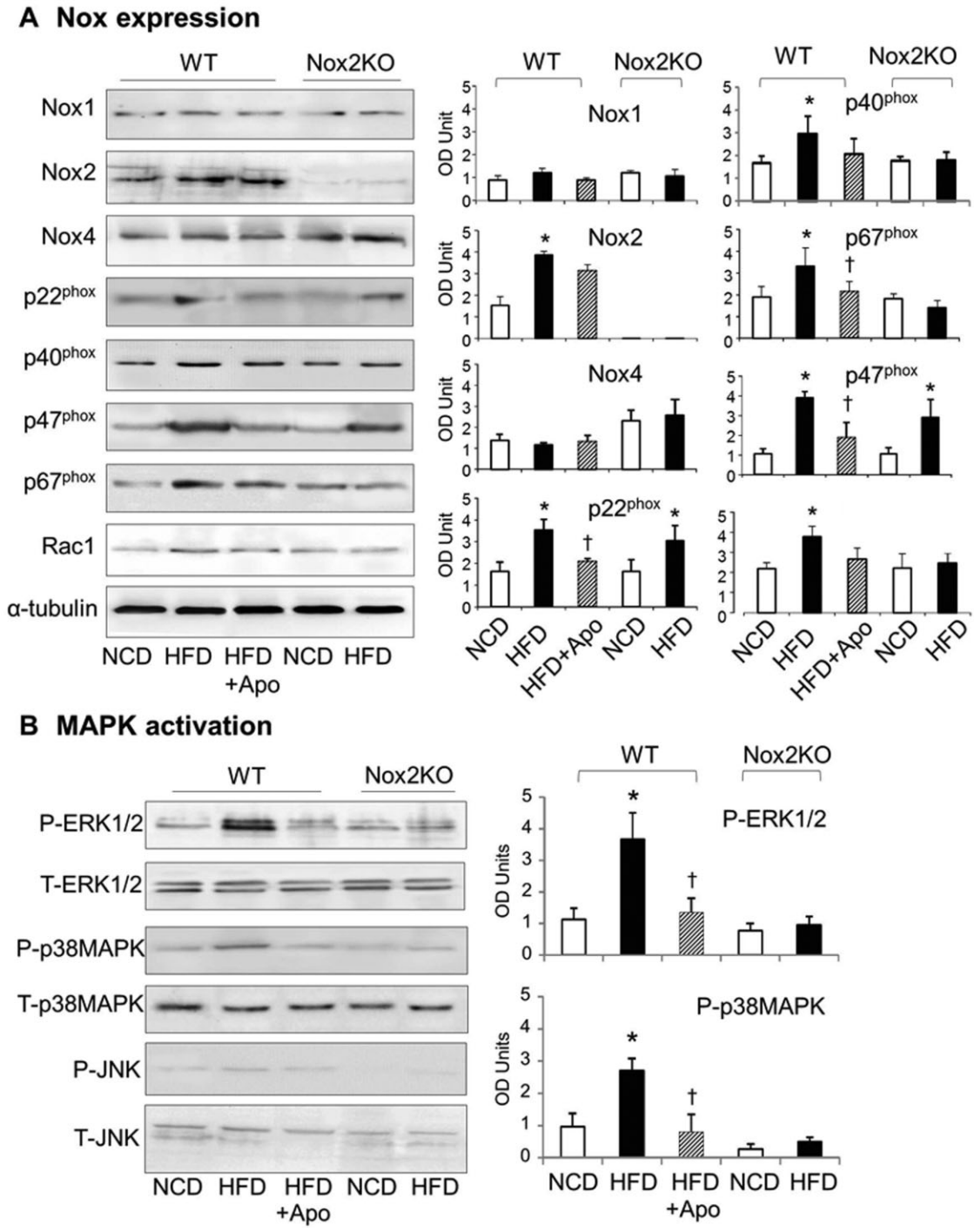

Figure 3

Nox expression and MAPK phosphorylation assayed by Western blot. (A) Levels of protein expression of Nox1, Nox2, Nox4, $p22^{phox}$, $p40^{phox}$, $p47^{phox}$, $p67^{phox}$ and Rac1. α-Tubulin detected in the same sample was used as a loading control. The optical densities (OD) of Nox subunit bands were quantified digitally and normalized to the α-tubulin levels. (B) Phosphorylation of ERK1/2, p38MAPK and JNK in aorta homogenates. The OD of the phospho-protein bands were quantified and normalized to the total protein levels of the same kinase detected in the same samples. *$P < 0.05$, significantly different from NCD values. †$P < 0.05$, significantly different from HFD values. $n = 9$ mice per group.

acetylcholine was completely abolished by L-NAME or endothelial denudation (Figure 4B), which further confirmed the relaxation was NO and endothelium dependent. There was no significant difference in relaxation of aortic rings to SNP, an endothelium-independent vasodilator indicating that the HFD effects were on the endothelium rather than on the smooth muscle cells (Figure 4B, lower left panel). The impairment of endothelium-dependent relaxation to

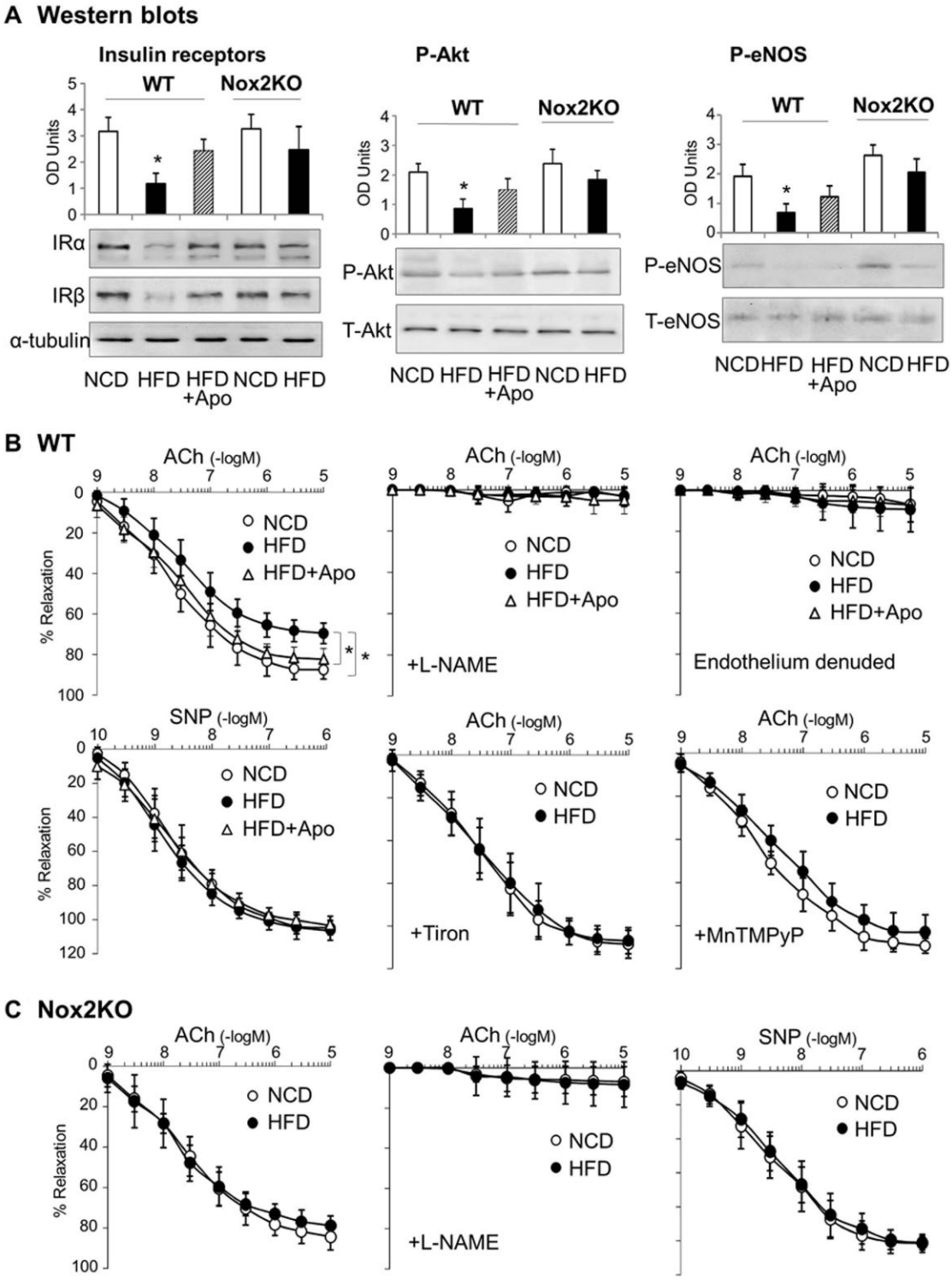

Figure 4

High-fat diet (HFD)-induced IR down-regulation and endothelial dysfunction in aortas of wild-type (WT) and Nox2KO mice. (A) Western blot assay of IR expression, and Akt and eNOS phosphorylation in aorta homogenates. For quantification, the optical densities (OD) of IRα and IRβ bands were quantified and normalized to the levels of α-tubulin detected in the same samples. For the quantification of phospho-Akt and phospho-eNOS, the optical densities (OD) of the phosphorylation bands were normalized to the total protein bands of the same protein in the same sample. (B) and (C) Endothelial-dependent and independent relaxation of aorta rings. *$P < 0.05$, significantly different from NCD values. $n = 10$ mice per group.

acetylcholine in HFD WT aorta was inhibited by tiron or Mn(III)tetrakis(1-methyl-4-pyridyl)porphyrin (MnTMPyP; Enzo Life Sciences, Exeter, UK) (a cell permeable SOD mimic), which further confirmed the role of ROS in mediating HFD-induced endothelial dysfunction (Figure 4B, lower middle and right panels). In contrast, endothelium-dependent relaxation to acetylcholine was well preserved in HFD-Nox2KO aortas, compared with their NCD controls (Figure 4C).

The relationship between Nox2-derived ROS production, IR expression and eNOS phosphorylation in aortas of WT and Nox2KO mice

Our data so far suggested that HFD-induced Nox2 activation and oxidative stress was the basis of the insulin resistance and vascular dysfunction. To further investigate this, we examined *in situ* $O_2^{\cdot-}$ production by vessel sections, using DHE fluorescence (Figure 5A). Experiments were performed in the presence or absence of tiron (an $O_2^{\cdot-}$ scavenger), and tiron-inhibitable $O_2^{\cdot-}$ production was quantified. HFD WT aortas had twofold more $O_2^{\cdot-}$ production than the NCD WT controls, and this was completely inhibited by apocynin treatment. In contrast, HFD failed to increase $O_2^{\cdot-}$ production by Nox2KO aortas. The integrity of aorta morphology was shown by haematoxylin and eosin (H&E) staining.

The relationship between Nox2 and vascular IRα expression was also examined by double-staining immunofluorescence on the same sections (Figure 5B). We found that HFD up-regulated the Nox2 expression significantly (red colour), mainly in the endothelium and the adventitia and very little in the media of smooth muscle cells, and this was accompanied by a significant reduction of IRα expression (green colour) throughout the vessel wall. However, in apocynin-treated WT or Nox2KO aortas, the levels of IRα expression were well preserved under HFD (Figure 5B). We also examined the relationship between Nox2 expression and eNOS phosphorylation, and found that along with the up-regulation of Nox2 expression (red colour), the levels of phospho-eNOS (green colour, a specific marker for the endothelium) were significantly reduced in HFD WT aortas (Figure 5C). Although eNOS phosphorylation was also reduced in apocynin-treated WT or Nox2KO aortas given the HFD, the reduction was not statistically significant, compared with NCD controls.

Relaxation of aortic rings in response to insulin, and ERK1/2 activation, IR expression and eNOS phosphorylation in aortic tissue stimulated by high glucose and insulin

In order to confirm that the relaxant effects of insulin were indeed reduced in HFD-treated mice, we pre-incubated aortas with or without insulin (1.2 nM) for 2 h and examined the contractile response of aortic rings to phenylephrine (0.001–10 μM added cumulatively). Compared to vehicle-treated vessels, pre-incubation of NCD WT aortas with insulin attenuated the contractile responses to phenylephrine (Figure 6A). In contrast, the relaxant response to insulin was abolished in aortas from HFD WT mice, and this was restored after apocynin treatment. Insulin-mediated relaxant responses were well maintained in aortas from Nox2 KO mice (Figure 6B).

The role of metabolic disorder-related Nox2 activation in damaging the function of vascular IR and the potential interaction between ERK1/2 activation and eNOS dysfunction were further examined by *ex vivo* culture of NCD aortas for 24 h with high levels of glucose (40 mM) plus insulin (1.2 nM), to mimic the condition of insulin resistance. We found that high glucose and insulin significantly increased the levels of Nox2 expression and ERK1/2 phosphorylation, and decreased the expression of IRα and eNOS phosphorylation in WT aortas (Figure 6C). Inhibition of ERK1/2 activation (with U0126) had no significant effect on high glucose and insulin-induced Nox2 and IRα expression, but preserved the levels of eNOS phosphorylation. Apocynin treatment preserved IRα expression and eNOS phosphorylation at control levels. All these high glucose and insulin-induced changes were absent in Nox2KO aortas.

Discussion and conclusion

Oxidative stress due to Nox2 activation has been recognized to play an important role in the development of cardiovascular complications in middle-aged patients suffering from obesity, insulin resistance and type 2 diabetes (Furukawa *et al.*, 2004; Sonta *et al.*, 2004). The current study used mice with an obesity-prone C57BL/6J background, at 11 months of age which is equivalent to a human age of about 50 years, when most cardiovascular diseases occur (Kim *et al.*, 2008; Houston *et al.*, 2009). Ageing *per se* has an important effect on ROS generation and vascular function and aged animals gained more weight on the HFD, than young animals (Erdos *et al.*, 2011). Therefore, the metabolic disorders and vascular oxidative stress reported here reflect the effects of both ageing and HFD. In addition to the metabolic syndrome described elsewhere, the novel discoveries from the current study are that (i) the HFD-induced Nox2 activation was associated with reduced vascular IR expression and profound endothelial dysfunction; and (ii) treatment of HFD WT mice with apocynin or Nox2KO preserved vascular IR expression and endothelial function, and reduced symptoms of the metabolic syndrome. There was a close link between HFD-induced Nox2 activation, insulin-resistance and weight gain, such that mice treated with apocynin or Nox2KO gained less body and fat weight than their littermates given the HFD. It is well known that Nox2 is crucial for phagocytic ROS production, and macrophage-mediated adipose inflammation plays a key role in the increased adipocyte size and body mass induced by HFD (Weisberg *et al.*, 2003; Lee *et al.*, 2011). Nox2 deficiency attenuated HFD-induced adipose deposits, adipocyte hypertrophy and adipose macrophage infiltration (Pepping *et al.*, 2013). Therefore, inhibition of inflammation and reduction of oxidative stress play an important role in the reduction of fat gain in apocynin-treated WT and Nox2KO mice given HFD, as there was no significant difference in food intake between groups given the same diet (Table 1). However, the development of obesity depends also on the balance between white adipose tissue (energy storage) and brown adipose tissue (energy expenditure) (Gesta *et al.*, 2007). It is also possible that inflammation and oxidative stress might promote white adipose tissue formation and obesity, whereas, inhibition or knockout of Nox2 might favour brown adipose tissue

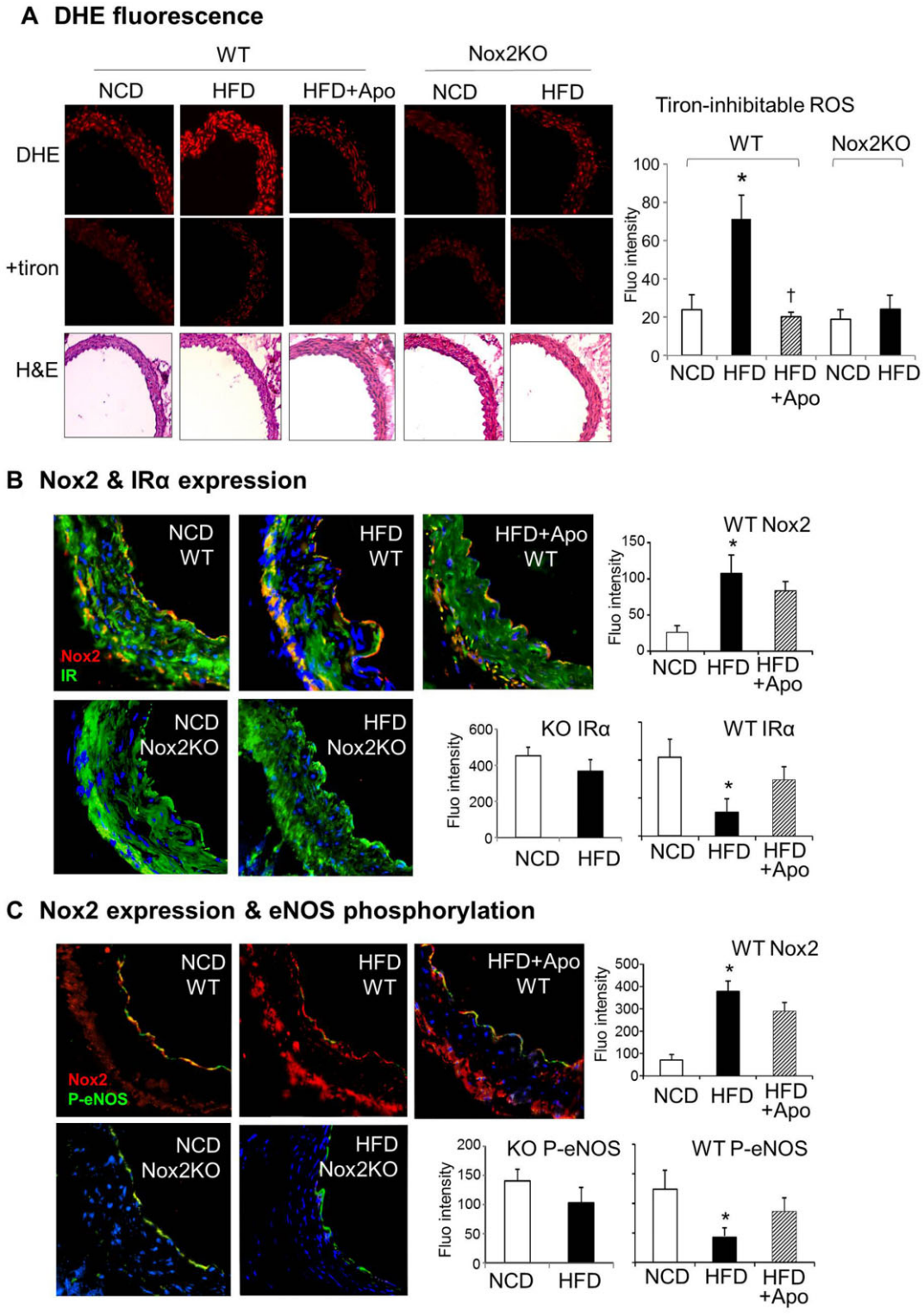

Figure 5

In situ detection of reactive oxygen species (ROS) production, IRα expression and eNOS phosphorylation in aortic sections of wild-type (WT) and Nox2KO mice. (A) ROS production detected by dihydroethidium (DHE) fluorescence microscope on aorta sections. Sections stained with H&E were used to show the aorta morphology. The fluorescence intensity was quantified and calculated for the tiron-inhibitable $O_2^{\cdot-}$ production. *$P < 0.05$, significantly different from normal chow diet (NCD) values; †$P < 0.05$, significantly different from high-fat diet (HFD) values. $n = 6$ mice per group. (B) Nox2 was labelled by Cy3 (red) and IRα was labelled by FITC (green) and nuclei was labelled by DAPI (blue). (C) Nox2 was labelled by Cy3 (red) and phospho-eNOS was labelled by FITC (green). The nuclei were labelled by DAPI (blue) in the Nox2KO aorta sections to visualize the vessel wall. The fluorescence intensity of individual molecule was quantified. *$P < 0.05$, significantly different from NCD values. $n = 6$ mice per group.

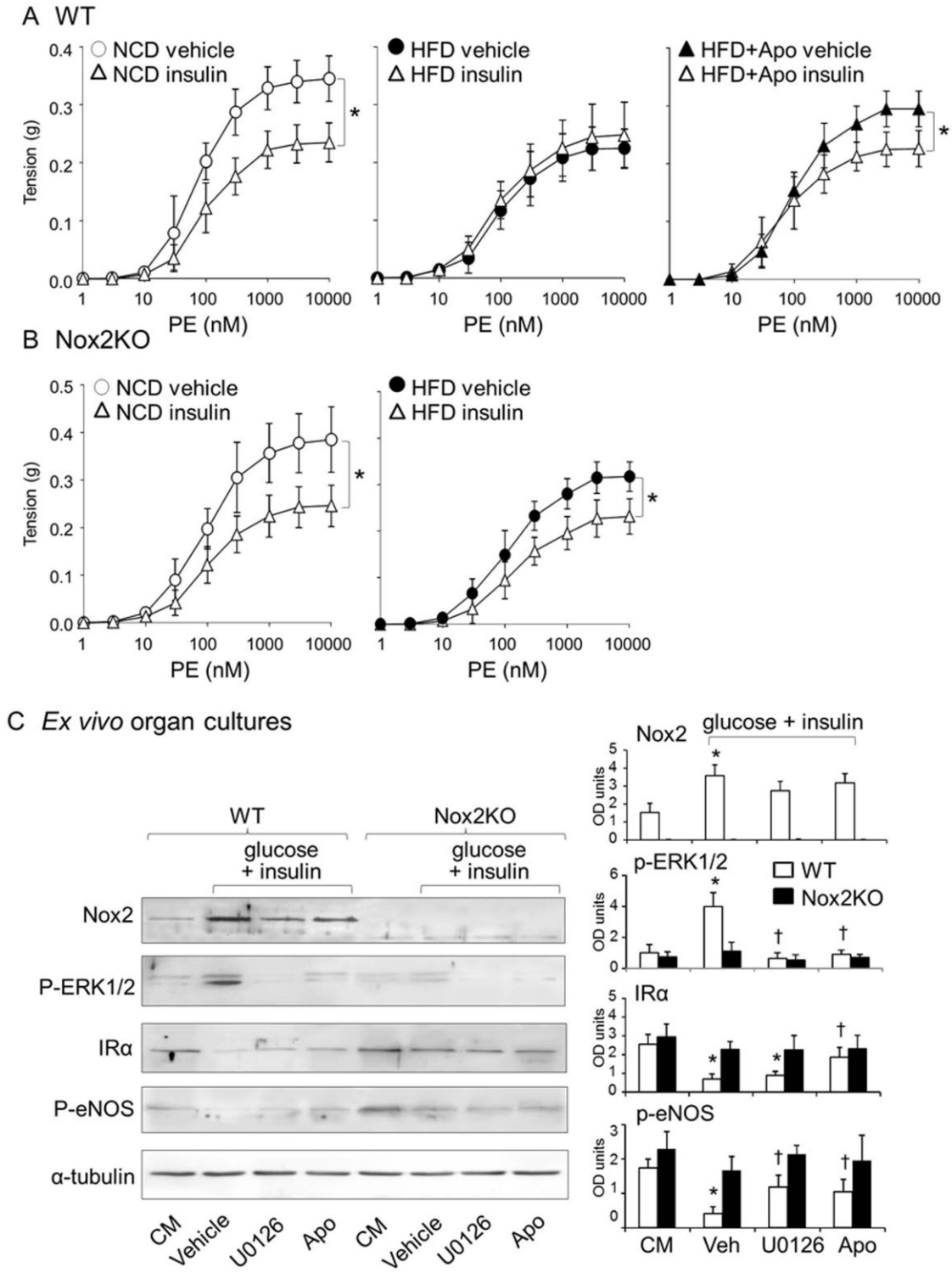

Figure 6

Aortic vasomotor response to insulin stimulation and *ex vivo* organ culture for insulin and high glucose-induced changes in insulin receptor (IR) expression, and ERK1/2 and eNOS phosphorylation. The effect of pre-incubation with insulin (1.2 nM for 2 h) on the contractile response to phenylephrine was assessed in aortic rings from (A) wild-type (WT) and (B) Nox2KO mice. *$P < 0.05$, significant effect of insulin; $n = 8$ mice per group. (C) Western blots. Aortic rings from normal chow diet (NCD) mice were cultured for 24 h in the control medium (CM, 2% FCS/DMEM), or stimulated with insulin (Ins, 1.2 nM) and glucose (Glu, 40 mM) and in the presence of vehicle or an inhibitor of ERK1/2 activation (U0126, 10 μM) or apocynin (Apo, 100 μM). The optical densities (OD) of Nox2, phospho-ERK1/2, IRα, and phospho-eNOS bands were quantified and normalized to the levels of α-tubulin detected in the same samples. *$P < 0.05$, significantly different from CM values. †$P < 0.05$, significantly different from vehicle (Veh) values, with high glucose and insulin stimulation. $n = 6$ mice per group.

formation and thermogenesis, which would reduce obesity. Another outcome of the current study was that the hyperinsulinaemia persisted in apocynin-treated WT and Nox2KO mice given HFD. This finding is supported by a recent report that Nox2 is a negative modulator for pancreatic insulin secretion and that islets from Nox2KO mice secreted significantly more insulin in response to high glucose stimulation than the WT controls (Li *et al.*, 2012).

Arteries and particularly the large arteries, develop atherosclerosis and stiffness with age and are more susceptible than other tissues to the deleterious effects of nutrient overload (Kim *et al.*, 2008). Mouse aorta is a well-established and frequently used model for studying HFD and aging-related oxidative stress and vascular dysfunction. Endothelial oxidative stress associated with Nox2 activation, preceded the pathogenesis of hypertension and atherosclerosis, two of the most common cardiovascular complications suffered by obese and diabetic patients (Evans *et al.*, 2002; Nigro *et al.*, 2006; Gupta *et al.*, 2012). In the current study using two independent techniques, lucigenin-chemiluminescence and *in situ* DHE fluorescence, we found that HFD WT aortas produced about twice as much ROS as the NCD controls and this was accompanied by profound endothelial dysfunction, characterized by reduced eNOS phosphorylation and NO production, and impaired endothelium function. Furthermore, the mice were hypertensive. The impaired vascular relaxation was related to oxidative damage, because addition of tiron or MnTMPyP in the organ bath restored the endothelial function. Furthermore, treating mice with apocynin or Nox2KO abolished HFD-induced vascular ROS production, preserved the eNOS and endothelial function and mice were normotensive. Although vascular iNOS might be involved in the HFD-induced endothelial dysfunction, knockout of iNOS provided no protection against HFD-induced oxidative stress and hypertension (Noronha *et al.*, 2005).

Among the Nox isoforms, Nox2 is mainly expressed in the endothelium and adventitia and is the predominant isoform up-regulated in obesity and HFD-induced vascular oxidative stress (Furukawa *et al.*, 2004). Although a previous study found up-regulation of Nox1 and Nox4 in aortas of WT mice under HFD, they used young (10 week old) mice and there were no symptoms of vascular oxidative stress and metabolic disorder associated after HFD-intervention (Cui *et al.*, 2009). In contrast to this previous study, mice used in the current study were 11 months old and HFD significantly increased Nox2 expression (but not that of Nox1 and Nox4) in aortas of WT mice, mainly in the endothelium and adventitia. It is possible that increased adventitial Nox2 expression may also come from inflammatory cell infiltration. Interestingly, apocynin treatment did not alter Nox2 expression, but inhibited HFD-induced increases in $p22^{phox}$, $p40^{phox}$, $p67^{phox}$ and $p47^{phox}$ and Rac1 expression. This, on the other hand, implied that the inhibitory effect of apocynin on HFD-induced $O_2^{\cdot-}$ production was indeed on the activity of Nox2 rather than the effect of an antioxidant.

Redox-sensitive MAPKs are important signalling pathways for both insulin and Nox2-derived ROS. MAPK activation, in particular ERK1/2 phosphorylation has been reported in the vasculature of animals suffering from dietary obesity and insulin resistance (Kim *et al.*, 2008; Symons *et al.*, 2009), as well as in endothelial cells isolated from patients with type 2 diabetes (Gogg *et al.*, 2009). Likewise, in the current study, we found a close relationship between ERK1/2 activation, impaired Akt/eNOS phosphorylation and endothelial dysfunction in HFD WT aortas, but not in aortas of apocynin-treated or HFD-Nox2KO mice. *Ex vivo* experiments further confirmed that inhibition of ERK1/2 activation by U0126 preserved eNOS phosphorylation, following high glucose and insulin stimulation.

Insulin through its receptors, IRα and IRβ, promotes vasodilation and plays an important role in regulating BP and vascular metabolism. Mice heterozygous for knockout of IR are hypertensive (Wheatcroft *et al.*, 2004), and mice with targeted vascular endothelial IR deficiency had reduced levels of eNOS expression (Sato *et al.*, 2005). One of the important findings in the current study is that HFD reduced significantly the expression of IR in the aortas of WT mice, as detected by both Western blot and immunofluorescence. Reduced IR expression was due to Nox2-derived oxidative stress and insulin resistance because inhibition of Nox2 by apocynin or Nox2KO improved insulin sensitivity and restored aortic IR expression. We also found that reduced IR expression was accompanied by decreased Akt activity in HFD WT mice.

It is well known that Nox2 activity (the oxidative burst) is crucial for neutrophil function and host defence against bacterial and fungal infection, and there is concern that targeting Nox2 may cause symptoms of chronic granulomatous disease. Our answer to that is although there is structural similarity between the neutrophil and endothelial Nox2 enzymes, there are profound biochemical and functional differences between them and that the regulatory mechanism of Nox2 activation is completely different in endothelial cells from that in neutrophils (Li and Shah, 2002). Targeting the mechanism specifically for endothelial Nox2 activation is a valid approach. On the other hand, even when it is fully activated, total endothelial Nox2 activity is only about 1% of that in the neutrophils (Drummond *et al.*, 2011). Thus, there is room for developing a specific Nox2 inhibitor that inhibits the activation of endothelial Nox2 at a low dose, which would not be enough to affect neutrophil Nox2 activity.

In summary, the current study reported for the first time that diet-induced obesity in middle-aged mice was linked with vascular Nox2 activation, oxidative damage to IR function and endothelial dysfunction. Targeting Nox2 represents an effective therapy to reduce dietary obesity-related oxidative stress, to increase insulin sensitivity and to improve vascular function.

Acknowledgement

J. D. was supported by the University of Surrey Overseas Research Student Award Scheme.

Conflict of interest

None.

References

Abudu N, Levinson SS (2007). Calculated low-density lipoprotein cholesterol remains a viable and important test for screening and targeting therapy. Clin Chem Lab Med 45: 1319–1325.

Bailey CJ (2011). The challenge of managing coexistent type 2 diabetes and obesity. BMJ 342: d1996.

Cui W, Matsuno K, Iwata K, Ibi M, Katsuyama M, Kakehi T *et al.* (2009). NADPH oxidase isoforms and anti-hypertensive effects of atorvastatin demonstrated in two animal models. J Pharmacol Sci 111: 260–268.

Drummond GR, Selemidis S, Griendling KK, Sobey CG (2011). Combating oxidative stress in vascular disease: NADPH oxidases as therapeutic targets. Nat Rev Drug Discov 10: 453–471.

Erdos B, Kirichenko N, Whidden M, Basgut B, Woods M, Cudykier I *et al.* (2011). Effect of age on high-fat diet-induced hypertension. Am J Physiol Heart Circ Physiol 301: H164–H172.

Evans JL, Goldfine ID, Maddux BA, Grodsky GM (2002). Oxidative stress and stress-activated signaling pathways: a unifying hypothesis of type 2 diabetes. Endocr Rev 23: 599–622.

Fan LM, Teng L, Li J-M (2009). Knockout of $p47^{phox}$ uncovers a critical role of $p40^{phox}$ in reactive oxygen species production in microvascular endothelial cells. Arterioscler Thromb Vasc Biol 29: 1651–1656.

Furukawa S, Fujita T, Shimabukuro M, Iwaki M, Yamada Y, Nakajima Y *et al.* (2004). Increased oxidative stress in obesity and its impact on metabolic syndrome. J Clin Invest 114: 1752–1761.

Gesta S, Tseng Y-H, Kahn CR (2007). Developmental origin of fat: tracking obesity to its source. Cell 131: 242–256.

Gogg S, Smith U, Jansson P-A (2009). Increased MAPK activation and impaired insulin signaling in subcutaneous microvascular endothelial cells in type 2 diabetes: the role of endothelin-1. Diabetes 58: 2238–2245.

Gupta AK, Ravussin E, Johannsen DL, Stull AJ, Cefalu WT, Johnson WD (2012). Endothelial dysfunction: an early cardiovascular risk marker in asymptomatic obese individuals with prediabetes. Br J Med Med Res 2: 413–423.

Heumüller S, Wind S, Barbosa-Sicard E, Schmidt HH, Busse R, Schröder K *et al.* (2008). Apocynin is not an inhibitor of vascular NADPH oxidases but an antioxidant. Hypertension 51: 211–217.

Hink U, Li H, Mollnau H, Oelze M, Matheis E, Hartmann M *et al.* (2001). Mechanisms underlying endothelial dysfunction in diabetes mellitus. Circ Res 88: E14–E22.

Houston DK, Nicklas BJ, Zizza CA (2009). Weighty concerns: the growing prevalence of obesity among older adults. J Am Diet Assoc 109: 1886–1895.

Kilkenny C, Browne W, Cuthill IC, Emerson M, Altman DG (2010). Animal research: reporting *in vivo* experiments: the ARRIVE guidelines. Br J Pharmacol 160: 1577–1579.

Kim F, Pham M, Maloney E, Rizzo NO, Morton GJ, Wisse BE *et al.* (2008). Vascular inflammation, insulin resistance, and reduced nitric oxide production precede the onset of peripheral insulin resistance. Arterioscler Thromb Vasc Biol 28: 1982–1988.

Lassègue B, Clempus RE (2003). Vascular NAD(P)H oxidases: specific features, expression, and regulation. Am J Physiol Regul Integr Comp Physiol 285: R277–R297.

Lee YS, Li P, Huh JY, Hwang IJ, Lu M, Kim JI *et al.* (2011). Inflammation is necessary for long-term but not short-term high-fat diet-induced insulin resistance. Diabetes 60: 2474–2483.

Li J-M, Shah AM (2002). Intracellular localization and pre-assembly of the NADPH oxidase complex in cultured endothelial cells. J Biol Chem 277: 19952–19960.

Li J-M, Shah AM (2004). Endothelial cell superoxide generation: regulation and relevance for cardiovascular pathophysiology. Am J Physiol Regul Integr Comp Physiol 287: R1014–R1030.

Li J-M, Mullen AM, Yun S, Wientjes F, Brouns GY, Thrasher AJ *et al.* (2002). Essential role of the NADPH oxidase subunit $p47^{phox}$ in endothelial cell superoxide production in response to phorbol ester and tumor necrosis factor-α. Circ Res 90: 143–150.

Li J-M, Wheatcroft S, Fan LM, Kearney MT, Shah AM (2004). Opposing roles of $p47^{phox}$ in basal versus angiotensin II-stimulated alterations in vascular O_2^- production, vascular tone, and mitogen-activated protein kinase activation. Circulation 109: 1307–1313.

Li J-M, Fan LM, Christie MR, Shah AM (2005). Acute tumor necrosis factor alpha signaling via NADPH oxidase in microvascular endothelial cells: role of $p47^{phox}$ phosphorylation and binding to TRAF4. Mol Cell Biol 25: 2320–2330.

Li N, Li B, Brun T, Deffert-Delbouille C, Mahiout Z, Daali Y *et al.* (2012). NADPH oxidase Nox2 defines a new antagonistic role for reactive oxygen species and cAMP/PKA in the regulation of insulin secretion. Diabetes 61: 2842–2850.

Lopez-Lopez JG, Moral-Sanz J, Frazziano G, Gomez-Villalobos MJ, Flores-Hernandez J, Monjaraz E *et al.* (2008). Diabetes induces pulmonary artery endothelial dysfunction by NADPH oxidase induction. Am J Physiol Lung Cell Mol Physiol 295: L727–L732.

McGrath J, Drummond G, McLachlan E, Kilkenny C, Wainwright C (2010). Guidelines for reporting experiments involving animals: the ARRIVE guidelines. Br J Pharmacol 160: 1573–1576.

Meng R, Zhu D-L, Bi Y, Yang D-H, Wang Y-P (2010). Apocynin improves insulin resistance through suppressing inflammation in high-fat diet-induced obese mice. Mediators Inflamm 2010: 858735.

Nigro J, Osman N, Dart AM, Little PJ (2006). Insulin resistance and atherosclerosis. Endocr Rev 27: 242–259.

Noronha BT, Li J-M, Wheatcroft SB, Shah AM, Kearney MT (2005). Inducible nitric oxide synthase has divergent effects on vascular and metabolic function in obesity. Diabetes 54: 1082–1089.

Oelze M, Knorr M, Schuhmacher S, Heeren T, Otto C, Schulz E *et al.* (2011). Vascular dysfunction in streptozotocin-induced experimental diabetes strictly depends on insulin deficiency. J Vasc Res 48: 275–284.

Parikh NI, Pencina MJ, Wang TJ, Lanier KJ, Fox CS, D'Agostino RB *et al.* (2007). Increasing trends in incidence of overweight and obesity over 5 decades. Am J Med 120: 242–250.

Pepping JK, Freeman LR, Gupta S, Keller JN, Bruce-Keller AJ (2013). Nox2 deficiency attenuates markers of adiposopathy and brain injury induced by high-fat diet. Am J Physiol Endocrinol Metab 304: E392–E404.

Sato A, Terata K, Miura H, Toyama K, Loberiza FRJ, Hatoum OA (2005). Mechanism of vasodilation to adenosine in coronary arterioles from patients with heart disease. Am J Physiol Heart Circ Physiol 288: H1633–H1640.

Silver AE, Beske SD, Christou DD, Donato AJ, Moreau KL, Eskurza I *et al.* (2007). Overweight and obese humans demonstrate increased vascular endothelial NAD(P)H oxidase-p47phox expression and evidence of endothelial oxidative stress. Circulation 115: 627–637.

Sonta T, Inoguchi T, Tsubouchi H, Sekiguchi N, Kobayashi K, Matsumoto S *et al.* (2004). Evidence for contribution of vascular

NAD(P)H oxidase to increased oxidative stress in animal models of diabetes and obesity. Free Radic Biol Med 37: 115–123.

Sukumar P, Viswambharan H, Imrie H, Cubbon RM, Yuldasheva N, Gage M *et al*. (2013). Nox2 NADPH oxidase has a critical role in insulin resistance-related endothelial cell dysfunction. Diabetes 62: 2130–2134.

Sumimoto H, Miyano K, Takeya R (2005). Molecular composition and regulation of the Nox family NAD(P)H oxidases. Biochem Biophys Res Commun 338: 677–686.

Symons JD, McMillin SL, Riehle C, Tanner J, Palionyte M, Hillas E (2009). Contribution of insulin and Akt1 signaling to endothelial nitric oxide synthase in the regulation of endothelial function and blood pressure. Circ Res 104: 1085–1094.

Teng L, Fan LM, Meijles D, Li J-M (2012). Divergent effects of p47phox phosphorylation at S303-4 or S379 on tumor necrosis factor-α signaling via TRAF4 and MAPK in endothelial cells. Arterioscler Thromb Vasc Biol 32: 1488–1496.

Thakur S, Du J, Hourani S, Ledent C, Li J-M (2010). Inactivation of adenosine A_{2A} receptor attenuates basal and angiotensin II-induced ROS production by Nox2 in endothelial cells. J Biol Chem 285: 40104–40113.

Touyz RM (2008). Apocynin, NADPH oxidase, and vascular cells: a complex matter. Hypertension 51: 172–174.

Violi F, Sanguigni V, Carnevale R, Plebani A, Rossi P, Finocchi A *et al*. (2009). Hereditary deficiency of gp91phox is associated with enhanced arterial dilatation: results of a multicenter study. Circulation 120: 1616–1622.

Weisberg SP, McCann D, Desai M, Rosenbaum M, Leibel RL, Ferrante AWJ (2003). Obesity is associated with macrophage accumulation in adipose tissue. J Clin Invest 112: 1796–1808.

Wheatcroft SB, Shah AM, Li J-M, Duncan E, Noronha BT, Crossey PA *et al*. (2004). Preserved glucoregulation but attenuation of the vascular actions of insulin in mice heterozygous for knockout of the insulin receptor. Diabetes 53: 2645–2652.

Yuan H, Lu Y, Huang X, He Q, Man Y, Zhou Y *et al*. (2010). Suppression of NADPH oxidase 2 substantially restores glucose-induced dysfunction of pancreatic NIT-1 cells. FEBS J 277: 5061–5071.